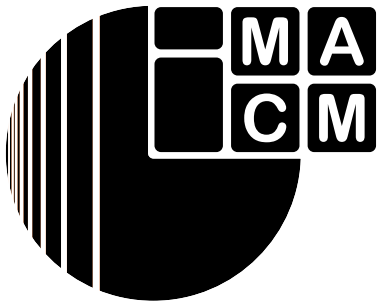

Bergische Universität Wuppertal

Fachbereich Mathematik und Naturwissenschaften

Institute of Mathematical Modelling, Analysis and Computational Mathematics (IMACM)

Preprint BUW-IMACM 13/27

Christian Hendricks and Matthias Ehrhardt

Evaluating the Effects of Changing Market Parameters and Policy Implications in the German Electricity Market

November 2013

http://www.math.uni-wuppertal.de

Evaluating the Effects of Changing Market Parameters and Policy Implications in the German Electricity Market

Christian Hendricks, Matthias Ehrhardt

Bergische Universität Wuppertal, Chair of Applied Mathematics and Numerical Analysis (AMNA), Gaußstrasse 20, 42119 Wuppertal, Germany

Abstract

In this paper we introduce a joint model for the electricity spot and the emission market in Germany. The model is used to simulate the effects of changing market parameters and policy implications. We propose a structural approach to connect fundamental factors, such as demand, capacity, fuel prices and emission allowances to the price of electricity. Based on empirical bid behaviour of electricity producers in day-ahead auctions we develop a novel CO_2 emission rate model. In order to introduce a feedback of CO_2 allowances to the actual emission of greenhouse gases a forward-backward stochastic differential equation is used to deduce a partial differential equation to price emission allowances. The resulting equation will be solved by an alternating direction implicit finite difference scheme.

[☆]The authors were supported in part by the European Union in the FP7-PEOPLE-2012-ITN Program under Grant Agreement Number 304617 (FP7 Marie Curie Action, Project Multi-ITN STRIKE - Novel Methods in Computational Finance).

Email addresses: hendricks@math.uni-wuppertal.de (Christian Hendricks), ehrhardt@math.uni-wuppertal.de (Matthias Ehrhardt)

1 Introduction

Over the course of the last two decades the liberalization of energy markets has accelerated in Germany. While in the past energy companies could act independently of competition with fixed prices, they now have to face variable prices. With the foundation of the Federal Network Agency, which guarantees grid access under fair conditions, the variety and quantity of market participants increased. This development led to more intense competition, also affecting fuel markets and the volatility of input costs. Since the installation of the *European Union Emission Trading System* (EU ETS) another impact factor has been introduced. As a power plant manager has to surrender enough *European Emission Allowances* (EUAs) to cover the emitted greenhouse gas, they can be interpreted as part of production costs, thus influencing the margin of a power plant. After the disaster in Fukushima the German federal government agreed on the abolishment of eight nuclear power plants and the transition to renewable energy. We see, that in opposition to the past, market participants now have to consider a more complex market situation and uncertainty about future price developments.

In this paper we want to analyse the effects of these developments in the German electricity market. We will investigate how changes of the main impact factors influence the spot price for electricity, the emission allowances and the value of conventional power plants. Beside renewable energy, coal and gas fired power plants form a major part of the German energy mix. The profitability of a certain plant will be determined by the spread between the price of one unit of electricity and its production costs. If we neglect operational constraints, such as starting and minimum operating times, a plant will be online whenever its spread is positive. Therefore, the value can be computed with the help of a real option approach, the so-called spread options.

The outline of this paper is as follows. In Section 2 clean spread options are defined, which are used to quantify the value of power plants. Section 3 deals with the German electricity spot market and its underlying impact factors. In the 4th Section the modelling framework to compute the market CO_2 emission rate and to price CO_2 allowances is introduced. In Section 5 we simulate several scenarios with our model and discuss the effects of changes in the key parameters.

2 Clean Spread Options

The value of a coal or gas fired power plant can be quantified with the help of clean dark spread options (coal) or clean spark spread options (gas). The spread determines the costs of transforming fuel into electricity at a given power plant efficiency. Clean options also take into account the costs of EUAs to offset the pollution of greenhouse gas.

In the following we define the spreads for the German market. The clean dark spread is defined as:

$$CDS = S - \tfrac{1}{e_{ff_1}} \left(K + e_1 A\right),$$

where S denotes the price of electricity in €/MWh, K the price of coal in €/MWh and A the price of an EUA in €/tCO_2. The variable e_1 determines how much greenhouse gas is emitted if one MWh of energy is produced at 100% efficiency. Corresponding to Abadie and Chamorro (2008), IPCC (2006) we set $e_1 = 0.34056$ tCO_2 / MWh. The power plant's efficiency is denoted by e_{ff_1}. It is the ratio between the produced output of energy and the needed input.

The clean spark spread is given by:

$$CSS = S - \tfrac{1}{e_{ff_2}} \left(G + e_2 A\right),$$

where G is the price of gas in €/MWh and e_2 the emission factor. According to Abadie and Chamorro (2008), IPCC (2006) the emission of natural gas is $e_2 = 0.20196$ tCO_2 / MWh. The efficiency of a gas fired power plant is denoted by e_{ff_2}.

The spread determines the economic value of a power plant. In an ideal world, with simplifying model assumptions, that there are neither delivery commitments nor restrictions on starting and minimum operating times of a power plant, it will be online whenever the spread is positive. Hence we can model its value by a call option on the spread with maturity T:

$$V_{CDS} = e^{-rT}\mathbb{E}\left(S_T - \frac{1}{e_{ff_1}}\left(K_T + e_1\, A_T\right)\right)^+, V_{CSS} = e^{-rT}\mathbb{E}\left(S_T - \frac{1}{e_{ff_2}}\left(G_T + e_2\, A_T\right)\right)^+.$$

If we consider a spread or exchange option between two assets, it is possible to price the option with a formula of Black and Scholes type. Margrabe (1978) was the first one, who derived this kind of formula. Since we want to include fundamental factors, such as demand and supply, we favour a structural model over a reduced form approach.

Figure 2.1 shows the peak hours (trading hours 9 to 20) spreads in the German electricity market during the year 2012. All data were taken from the *European Energy Exchange* (EEX). Since the coal price is quoted in USD / t, we transform it from t to MWh under the assumption that hard coal burns at a rate of 7.00126 MWh / t as reported by Heizung-Direkt (2013). With the help of the exchange rate from USD to €, we receive the desired quotation. The gas price is already quoted in €/ MWh and no further transformation is necessary. Corresponding to a study by the VDI (2007) we choose the typical efficiency of a coal fired plant as $e_{ff_1} = 41.425\%$ and of a gas fired one as $e_{ff_2} = 50.625\%$. The clean dark spread was always higher than the clean spark spread. This indicates that the average coal fired power plant was more profitable than the average gas fired power plant in 2012. In fact, the clean spark spread was negative most of the time and therefore, it was not profitable to produce energy with a gas fired plant. The plot reveals that there is a strong positive correlation between the spread of coal/gas power plants and the price of electricity.

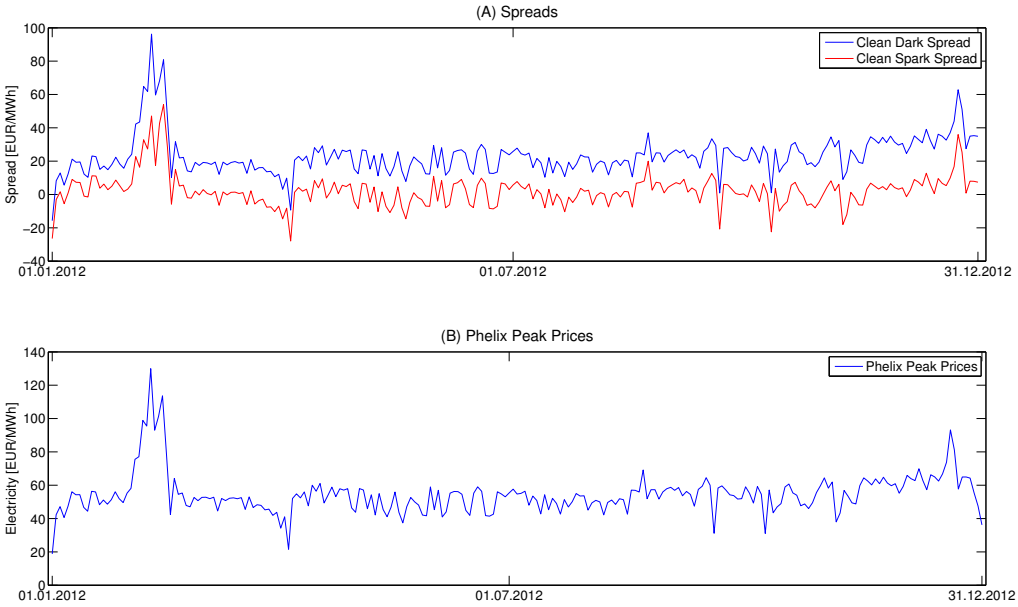

Figure 2.1: Spreads in the German electricity spot market (Peak hours)

3 The Electricity Spot Price

Since the liberalization of energy markets gathered pace, the number of modelling approaches has grown rapidly. They range from full equilibrium models to reduced form models. Equilibrium models try to identify all necessary parameters and economic fundamentals, which influence the price of energy. Therefore a huge amount of data and knowledge about all generating units, maintaining schedules, transmission constraints etc. is essential. On the one hand, these models provide deep insights into market mechanisms, but on the other hand, the tremendous amount of required data and its complexity make them unsuitable for derivatives pricing. For more details on equilibrium models we refer to Eydeland and Wolyniec (2002), Bessembinder and Lemmon (2002). Reduced form models approximate the energy price directly through stochastic processes. They are easy to use for straightforward derivatives pricing, but do not incorporate any fundamental factors. The most advanced models of this group include regime switching and jumps, in Culot et al. (2013) and DeJong (2006). Structural models try to combine the advantages of the two other approaches while avoiding their disadvantages. They focus on identifying and modelling the main price drivers (e.g. demand, supply, price of resources) and derive the energy price from them. Within this paper we want to propose a hybrid approach, which is less complex than equilibrium models, but still allows for fundamental drivers and their link to the price for electricity.

Howison and Coulon (2009) used a joint distribution function to extract bid curves by generator type (coal, gas) from historical bid data. They were able to show a mapping between densities' parameters and fundamental drivers, such as fuel prices. In the following section we will briefly review their approach.

3.1 Stochastic Bid Curves and the Price for Electricity

We consider a market at time t with a demand D_t for energy and a capacity C_t in MWh. During day ahead auctions energy companies place m bids, consisting of quantity q_j and price p_j for $j = 1, \cdots, m$. These bids are arranged in merit order and the market operator calls upon generators until the current demand is met. Let the distribution function $F_i(S_t)$ denote the proportion of bids below S_t €/MWh for generators of fuel type $i = 1, \cdots, n$, then the spot price S_t solves the equation

$$F(S_t) = \sum_{i=1}^{n} w_i F_i(S_t) = \tfrac{D_t}{C_t}, \text{ where } \sum_{i=1}^{n} w_i = 1.$$

Hence the electricity spot price can be expressed by

$$S_t = B(\tfrac{D_t}{C_t}) := F(.)^{-1}(\tfrac{D_t}{C_t}),$$

where $B : [0,1] \to \mathbb{R}$. Howison and Coulon (2009) suggest to use logistic distributions. To improve the goodness of fit they use a truncated domain with fixed lower and upper bounds b_L, b_U, where $b_L < \frac{D_t}{C_t} < b_U$ must hold. The demand and capacity can then be rescaled by

$$\hat{D}_t := D_t - b_L\, C_t, \qquad \hat{C}_t := (b_U - b_L)\, C_t.$$

Hence the spot price fulfills

$$F(S_t) = \sum_{i=1}^{n} w_i F_i(S_t) = \tfrac{\hat{D}_t}{\hat{C}_t}. \tag{3.1}$$

3.2 The German Spot Market

The German electricity market is relatively unique in the world. In the year 2000 the federal government passed the Renewable Energy Law (Erneuerbare Energiengesetz, EEG), which guarantees fixed prices for green power and their preferred feed-in. This has led to a steady increase of installed capacities of green energy. The Federal Ministry for the Environment, Nature Conservation and Nuclear Safety BMU (2004) estimates that renewable energy will represent 55% of the installed capacity in 2050. Today, solar and wind power are the most important contributors to green energy. However their production is significantly determined by the actual weather conditions. The combination of the great share of green power in the German energy mix and volatile production capacities makes the German market rather complicated.

In the following we want to analyse the demand and supply situation in the German market. We will use Phelix price data from the two last years.[1] It is traded at the EPEX Spot and published as Phelix Base and Phelix Peak. We cite from EPEXSpot (2012) the two definitions:

- **Phelix Day Base** is the average price of the hours 1 to 24 for electricity traded on the spot market. It is calculated for all calendar days of the year as the simple average of the auction prices for the hours 1 to 24 in the market area Germany disregarding power transmission bottlenecks.
- **Phelix Day Peak** is the average price of the hours 9 to 20 for electricity traded on the spot market. It is calculated for all calendar days of the year as the simple average of the auction prices for the hours 9 to 20 in the market area Germany disregarding power transmission bottlenecks.

During daily day ahead auctions bids ranging from -3000 € to 3000 € for each individual hour can be made. All bids are sorted by price and aggregate bids form the bid curve. Based on these results the energy price is calculated as the match of the bid and demand curve. In Figure 3.1 we see aggregated bid curves in the Phelix Energy market. In the German market huge bids at the lower bound of -3000 € can be observed. These bids represent renewable energies. Since the EEG forces to prefer renewable to conventional energy, their bids can be found at the lower bound of the price range. In Figure 3.2 we compare the quantity of bids below -1000 € to wind, solar production forecasts and to capacities from nuclear power plants. Please note that the capacities from nuclear power plants have also been added. Since they cannot be switched on or off easily and their running costs remain rather stable, regardless whether they are online or not, we assume their available capacity on the left hand side of the price range.The plots confirm that these bids can reasonable be explained by bids of wind, solar and nuclear power generators.

On the contrary to the original stochastic approach by Howison and Coulon (2009), we use variable bounds to account for changing bid volumes of clean generators:

$$b_L = \frac{\sum_{i=1}^{m} q_i \mathbb{1}_{\{p_i < -1000\}}}{\sum_{i=1}^{m} q_i}, \qquad b_U = 1 - \frac{\sum_{i=1}^{m} q_i \mathbb{1}_{\{p_i > 1000\}}}{\sum_{i=1}^{m} q_i}.$$

Beside renewable and nuclear energy, the German energy mix is dominated by coal (hard coal, lignite) and gas (gas, oil). After the bids of clean generators have been removed, the remaining ones belong to conventional generators. According to a study by the BDEW (2011) we set $w_1 = 0.6984$ (market capacity coal) and $w_2 = 0.3016$ (market capacity gas). In Figure 3.3 we compare the density parameters $\{\mu_1, \sigma_1\}$ of coal and $\{\mu_2, \sigma_2\}$ of gas generators to historical coal and gas prices. The parameters have been estimated with Maximum Likelihood Estimation using

[1] Phelix denotes the Physical Electricity Index in the German/Austrian market.

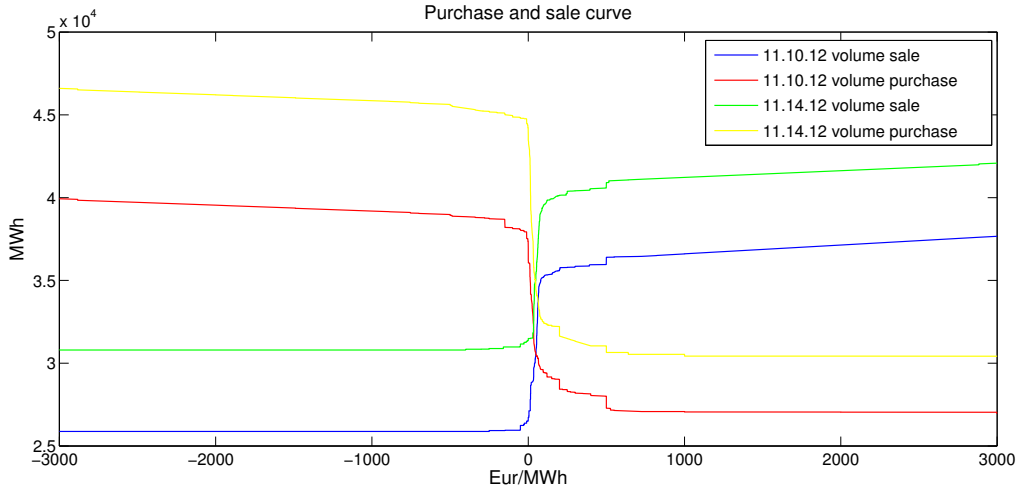

Figure 3.1: Phelix purchase and sale curve on 10th and 14th November 2012

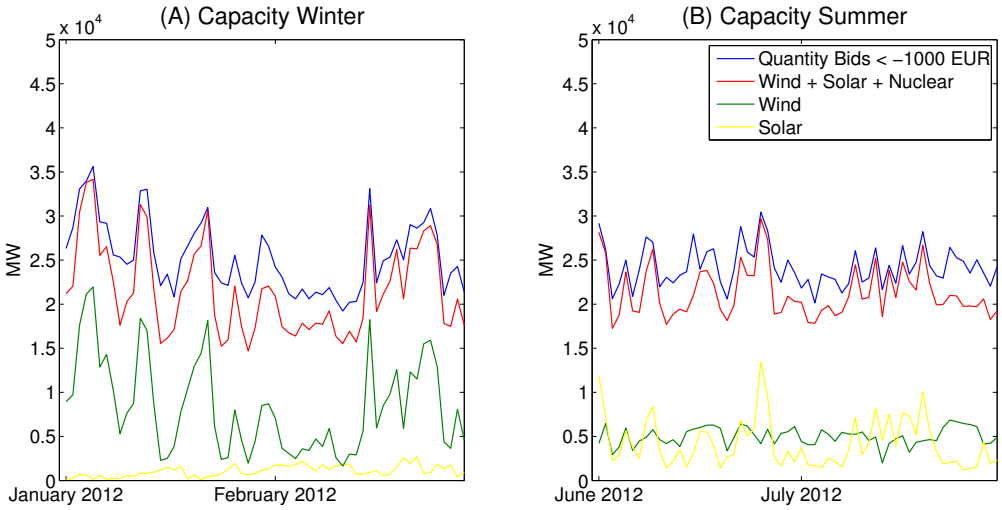

Figure 3.2: Quantity of bids below -1000 € and production forecasts

logistic density functions with expectation μ_i and standard deviation σ_i for $i = 1, 2$. The coal time series consists of future contracts with the nearest expiry. The gas price series is given by GASPOOL spot price data. The fitted parameters are correlated to coal and gas prices. Generators move their bids in accordance to changing production costs. In order to account for generators, which take the fuel prices and the assumed bid levels of the competing technology into consideration, we model the parameters with the help of a multiple linear regression model:

$$\mu_1 = \alpha_0 + \alpha_1 K + \alpha_2 G, \qquad \sigma_1 = \beta_0 + \beta_1 K + \beta_2 G,$$
$$\mu_2 = \gamma_0 + \gamma_1 K + \gamma_2 G, \qquad \sigma_2 = \delta_0 + \delta_1 K + \delta_2 G,$$

where K represents the price of coal, while G is the gas price. Table 3.1 shows the parameters, which were estimated via conditional (non-negative slopes) least square regression. The densities' parameters of coal generators have a positive sensitivity regarding the price for gas. As they precede gas generators in the supply stack (in our time series), they can move their bid levels upwards to gain an extra profit if the production costs of gas generators rise.

The R^2 values for our linear model show that there is a linear relationship between fuel prices and the densities' parameters. Although the values can only explain up to 22.93% of the variability,

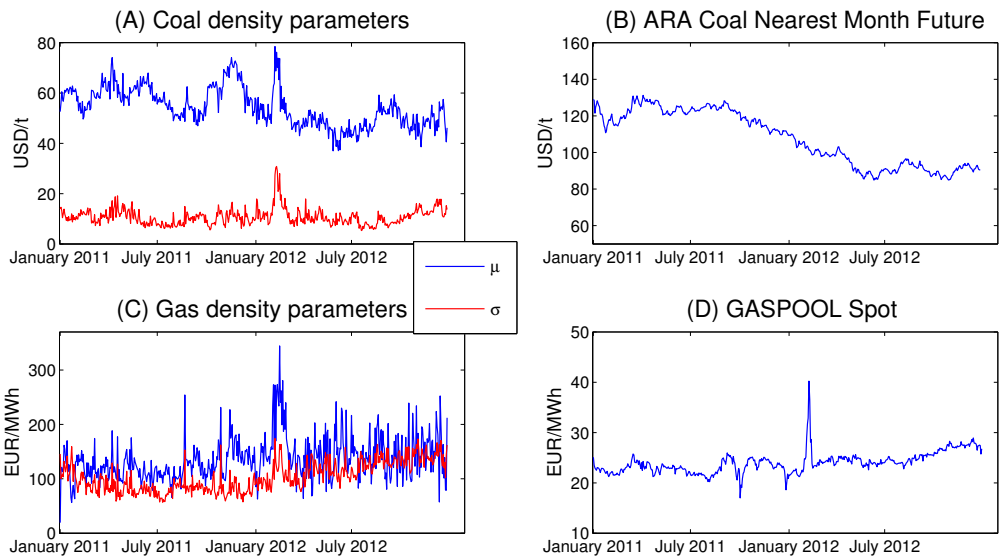

Figure 3.3: Fitted parameters and commodity prices

the p-value of the F-test (constant vs. regression model) indicates a significant linear relationship.

The spot price for energy S_t, in the case of logistic density functions, can now be calculated by solving equation (3.1)

$$B^{-1}(.)(S_t) = w_1 \frac{1}{1+e^{-\frac{S_t-(\alpha_0+\alpha_1 K+\alpha_2 G)}{\beta_0+\beta_1 K+\beta_2 G}}} + w_2 \frac{1}{1+e^{-\frac{S_t-(\gamma_0+\gamma_1 K+\gamma_2 G)}{\delta_0+\delta_1 K+\delta_2 G}}} = \frac{\hat{D}_t}{\hat{C}_t}\,. \tag{3.2}$$

The equation possesses no analytic solution and hence must be solved numerically.

	Intercept	Slope Coal	Slope Gas	R^2	p-Value (F-test)
μ_1	-27.69	0.3590	1.9285	0.2293	2.8800e-28
σ_1	-39.4864	0.1419	1.5298	0.2136	3.9257e-26
μ_2	-52.5649	0	7.7496	0.0860	3.5620e-11
σ_2	-59.1102	0	6.8472	0.1955	7.2888e-25

Table 3.1: Results by conditional regression

3.3 Demand and Capacity

The demand process D_t is not directly observable in auction data. To be able to use the framework presented before, we set D_t to the point of intersection of the sale and bid curve for every hour. The residual demand process $\hat{D}_t$ can be calculated via the transformation $\hat{D}_t = D_t - b_{L,t}C_t$. It can be interpreted as the demand, which has to be fulfilled by conventional generators. The process $\hat{C}_t$ can be derived from C_t by $\hat{C}_t = (b_{U,t} - b_{L,t})C_t$ and understood as the capacity of conventional generators. Figure 3.4 shows that most intra-day effects of $\hat{D}_t$, $\hat{C}_t$ are compensated by the patterns of D_t, C_t and $b_{L,t}$. In order to be able to model the intra-day and annual pattern

we model $\hat{D}_t$ as the sum of an Ornstein-Uhlenbeck process X_t and a seasonal component s_1

$$\begin{aligned} \log(\hat{D}_t) &= X_t + s_1(t) \\ dX_t &= \theta_1(\mu_1 - X_t)dt + \sigma_1 dW_t \\ s_1(t) &= \alpha_0 + \alpha_1 \cos\left(\frac{2\pi}{365*24}(t+\phi_1)\right) + \alpha_2 \cos\left(\frac{2\pi}{12}(t+\phi_2)\right) . \end{aligned} \tag{3.3}$$

To ensure that $0 < \hat{D}_t < \hat{C}_t$ always holds, we do not simulate the capacity directly, but the margin M_t and receive $\hat{C}_t$ via $\hat{C}_t = \hat{D}_t + M_t$. M_t can be interpreted as the "unused capacity" in the market. Therefore modelling $\hat{C}_t$ reduces to modelling a strictly positive process M_t. The process $\log(M_t)$ is

$$\begin{aligned} \log(M_t) &= Z_t + s_2(t) \\ dZ_t &= \theta_2(\mu_2 - Z_t)dt + \sigma_2 d\tilde{W}_t \\ s_2(t) &= \beta_0 + \beta_1 \cos\left(\frac{2\pi}{365*24}(t+\omega_1)\right) + \beta_2 \cos\left(\frac{2\pi}{24}(t+\omega_2)\right) . \end{aligned} \tag{3.4}$$

Figure 3.4 shows the averaged demand, capacity and margin time series. The unscaled demand

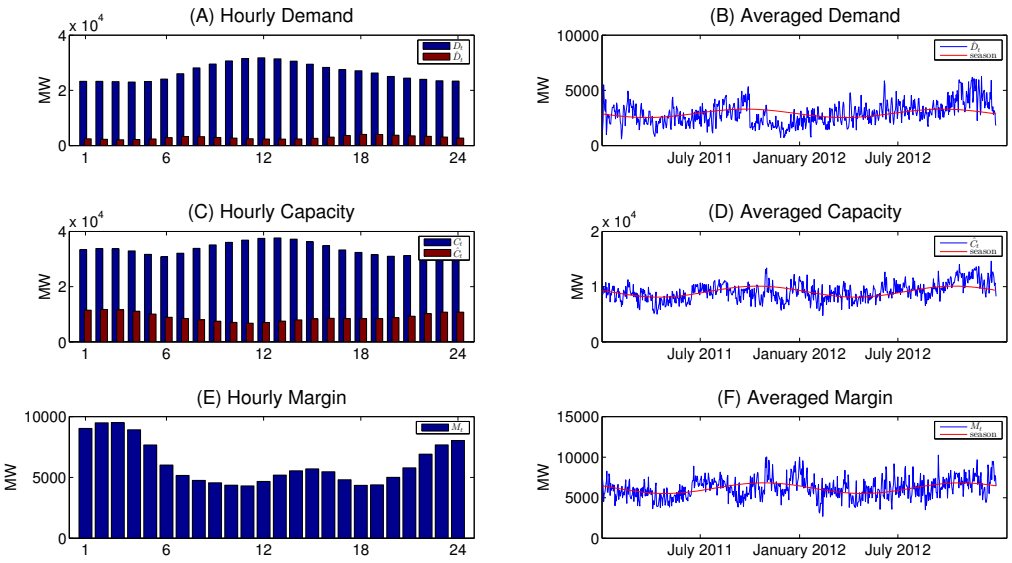

Figure 3.4: Hourly and daily demand, capacity and margin

process reaches its daily peak during midday, while the residual demand process exhibits one peak around 8 am and another one around 7 pm. We therefore use 2π / 12 as the period to model the intra-day pattern. Peaks in the morning and the early evening can also often be observed in intra-day Phelix spot data. The capacity shows the same pattern as the demand process. This may be explained by power plant maintaining schedules, which are designed to meet low demand times, so that most capacity is available when demand is at a high level. The scaled capacity process is highest in the night and reaches its low at midday. The margin process is highest during the night hours, when demand reaches its lows. Throughout the year a moderate annual pattern can be seen. Demand, capacity and margin are highest during autumn/winter and lowest in spring and summer.

The parameters in Table 3.2 have been estimated via least squares regression and the ones in Table 3.3 with Maximum Likelihood Estimation.

α_0	α_1	α_2	ϕ_1	ϕ_2
7.9544	0.0147	-0.2204	0.6520	-1.6143
β_0	β_1	β_2	ω_1	ω_2
8.6685	0.0488	0.3193	1.8095	-1.5501

Table 3.2: Seasonal parameters $\log(\hat{D}_t)$, $\log(M_t)$, cf. (3.3),(3.4)

i	θ_i	μ_i	σ_i
1	0.1304	-0.0017	0.2729
2	0.1641	-0.0007	0.2065

Table 3.3: Parameters X_t, Z_t, cf. (3.3),(3.4)

3.4 Gas and Coal

The fuel processes K_t, G_t are modelled with two correlated Ornstein-Uhlenbeck processes. In our data set no clear seasonal pattern can be observed. So we drop a seasonal component.

$$\begin{aligned} \log(K_t) &= Q_{1,t}, \\ dQ_{1,t} &= \theta_{Q_1}(\mu_{Q_2} - Q_{1,t})dt + \sigma_{Q_1}dW_{1,t}, \quad Q_{1,0} = q_{1,0} \in \mathbb{R}_+, \\ \log(G_t) &= Q_{2,t}, \\ dQ_{2,t} &= \theta_{Q_2}(\mu_{Q_2} - Q_{2,t})dt + \sigma_{Q_2}dW_{2,t}, \quad Q_{2,0} = q_{2,0} \in \mathbb{R}_+, \end{aligned} \tag{3.5}$$

where $dW_{1,t}dW_{2,t} = \rho dt$. In Figure (3.5) we computed the correlation of log-returns during 2008 to 2012. The plot makes clear that correlation changes over time and is not stable. This has also been addressed in literature, e.g. by Teng et al. (2013), who propose to use a stochastic correlation model. However, for tractability reasons we will consider a stable correlation in our simulations. We use the observed correlation $\rho = 0.0872$ of the years 2011 and 2012. Table 3.4 shows the estimated parameters of the logarithmic fuel time series.

i	θ_{Q_i}	μ_{Q_i}	σ_{Q_i}
1	0.00004	4.8598	0.0021
2	0.0026	3.219	0.007

Table 3.4: Parameters $Q_{1,t}$, $Q_{2,t}$, cf. (3.5)

3.5 Renewable Power

Renewable energies, such as solar and wind power, are directly feed-in and therefore have a strong impact on the price of electricity. In the following we want to model the capacities provided by solar and wind power. The employed data consists of historic feed-ins of the years 2011 and 2012, available at www.transparency.eex.com. Figure 3.6 shows the yearly and intra-day pattern of solar energy. It follows the cycle of the sun and lasts from sunrise to sunset and reaches its peak during midday. In the night it drops to a value of zero. In the summer the feed-in is stronger than in winter since there a more sunshine hours and the sun is more powerful. To account for this complex pattern, we proceed as follows: We model the logarithm of total daily capacity

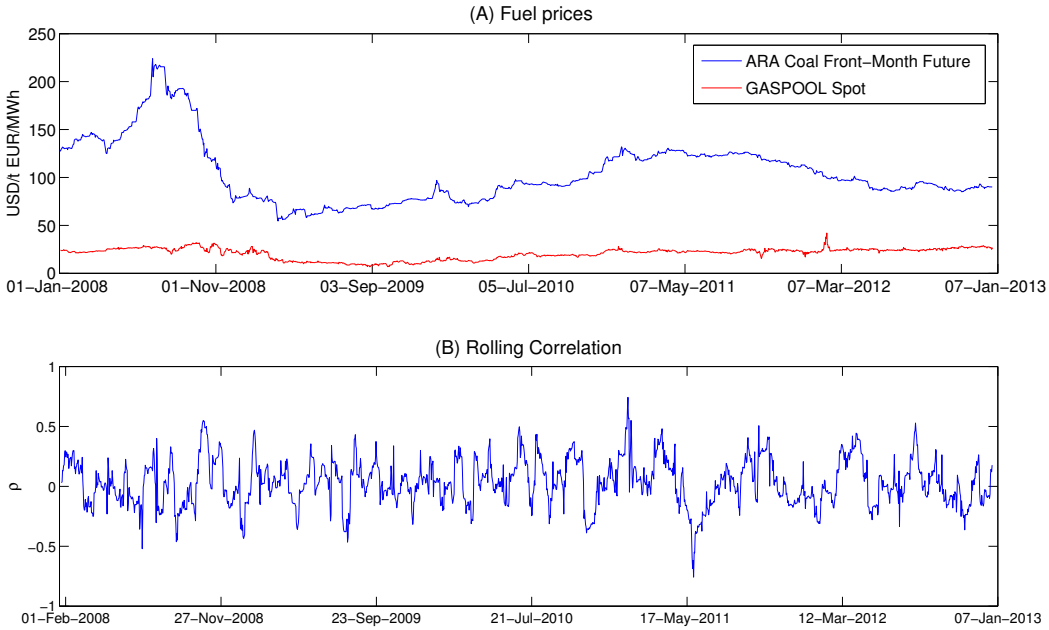

Figure 3.5: 20 days rolling window correlation

$\overline{I}^{solar}_{t_d}$ at day t_d as the sum of a stochastic and a deterministic, seasonal component

$$\begin{aligned} \log(\overline{I}^{solar}_{t_d}) &= E^{solar}_{t_d} + s_3(t_d) \\ dE^{solar}_{t_d} &= \theta_1(\mu_1 - E^{solar}_{t_d})dt_d + \sigma_1 dW_{t_d} \\ s_3(t_d) &= \alpha_0 + \alpha_1 \cos\left(\frac{2\pi}{365}(t_d + \phi_1)\right). \end{aligned} \tag{3.6}$$

The seasonal component captures the annual cycle. In order to receive hourly data, we propose to use the following transformation function, $\nu_{t_d} : \{t_d = 1, ..., 365\} \times \mathbb{R}^+_0 \to \mathbb{R}^+_0$

$$\nu_{t_d}(i, x) = x \sum_{j=1}^{24} c_j^{t_d} \mathbb{1}_{\{i\}}(j)$$

with $\sum_{j=1}^{24} c_j^{t_d} = 1$ for hours $i = 1, ..., 24$ of day t_d. The parameters c_j are calibrated to each day of the year and can be computed by dividing the hourly feed-in by the total daily feed-in. Since our time series consists of two years, we take the average of both years. The function ν_{t_d} distributes the total feed-in to the single hours of the day. Hence the feed-in at day t_d and hour i is given by

$$I^{solar}_{t_d,i} = \nu_{t_d}(i, \exp[E^{solar}_{t_d} + s_3(t_d)]). \tag{3.7}$$

In Figure 3.7 the wind feed-in of the year 2012 is plotted. The intra-day pattern exhibits a peak in the afternoon and declines until sunrise. This cycle is caused by the sun, which heats up the air and leads to air movement between warm and cold layers in the atmosphere. We split the time series into two components. The stochastic part models the random movement, while the

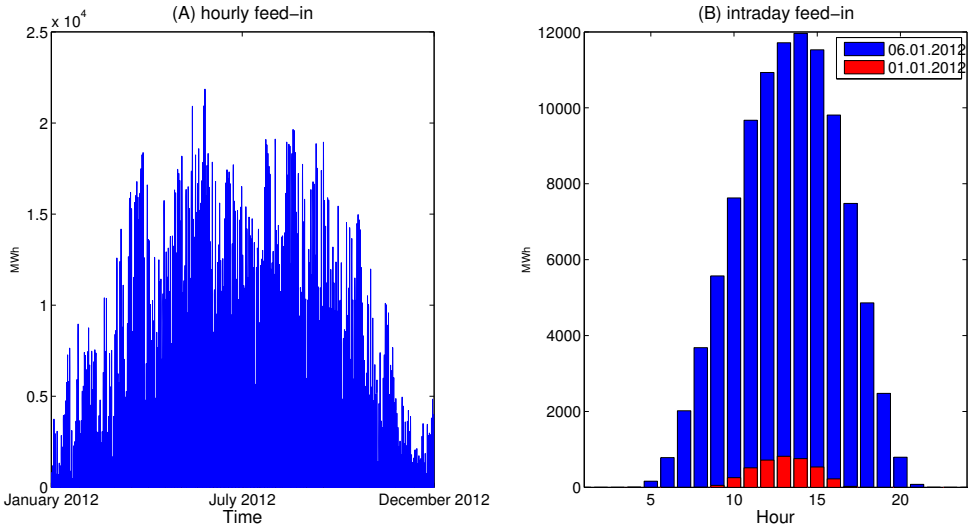

Figure 3.6: Solar power feed-in

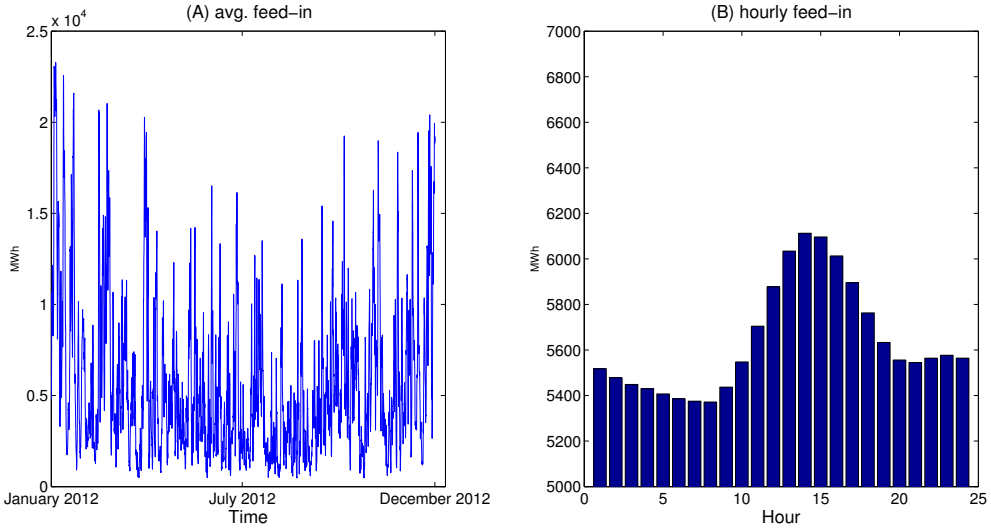

Figure 3.7: Wind power feed-in

seasonal component is deterministic and captures the annual and intra-day seasonality

$$\begin{aligned}\log(I_t^{wind}) &= E_t^{wind} + s_4(t)\\ E_t^{wind} &= \theta_2(\mu_2 - E_t^{wind})dt + \sigma_2 d\tilde{W}_t\\ s_4(t) &= \beta_0 + \beta_1 \cos\left(\frac{2\pi}{365*24}(t+\omega_1)\right) + \beta_2 \cos\left(\frac{2\pi}{24}(t+\omega_2)\right) + \beta_3 \cos\left(\frac{2\pi}{12}(t+\omega_3)\right).\end{aligned} \tag{3.8}$$

Tables 3.5 and 3.6 show the fitted parameters.

	θ_i	μ_i	σ_i
E^{solar}	0.3979	0.0120	0.1919
E^{wind}	0.0058	0.0055	0.0848

Table 3.5: Parameters E^{solar}, E^{wind}, cf. (3.6), (3.8)

α_0	α_1	ϕ_1				
10.7792	-1.026	4.7675				
β_0	β_1	β_2	β_3	ω_1	ω_2	ω_3
8.2896	0.3473	0.0379	-0.0234	-1.5925	4.9348	3.2682

Table 3.6: Seasonal parameters $\log(\overline{I}_{t_d}^{solar})$, $\log(I_t^{wind})$, cf. (3.6), (3.8)

3.6 Transformation

We used the logarithm of prices in (3.3) - (3.5). As we want to price derivatives with them, we have to transform them to Itô processes. We will do this for the demand and coal process. The application to the other ones is straight forward. Using (3.3) and the ansatz $\hat{D}_t := f(t, X_t) = e^{X_t + s_1(t)}$ we apply *Itô's Lemma* and obtain

$$\begin{aligned}d\hat{D}_t &= \left(e^{X_t+s_1(t)}\theta(\mu_1 - X_t) + s_1'(t)e^{X_t+s_1(t)} + \frac{1}{2}e^{X_t+s_1(t)}\sigma_1^2\right)dt + e^{X_t+s_1(t)}\sigma_1\, dW_t\\ &= \left(\theta\left[\mu_1 - \log(\hat{D}_t) + s_1(t)\right] + s_1'(t) + \frac{1}{2}\sigma_1^2\right)\hat{D}_t\, dt + \hat{D}_t\sigma_1 dW_t.\end{aligned} \tag{3.9}$$

For (3.5) we use $K_t := f(t, Q_t) = e^{Q_t}$ and *Itô's Lemma* yields

$$\begin{aligned}dK_t &= \left(e^{Q_{1,t}}\theta_{Q_1}\left[\mu_{Q_1} - Q_t\right] + \frac{1}{2}e^{Q_{1,t}}\sigma_{Q_1}^2\right)dt + e^{Q_{1,t}}\sigma_Q\, dW_t\\ &= \left(\theta_{Q_1}\left[\mu_{Q_1} - \log(K_t)\right] + \frac{1}{2}\sigma_{Q_1}^2\right)K_t\, dt + K_t\sigma_{Q_1}\, dW_t.\end{aligned} \tag{3.10}$$

4 European Emission Trading System

The *European Union Emission Trading System* (EU ETS) was launched in 2005 to reduce the emission of greenhouse gas. The 31 participants (27 EU member states and Croatia, Iceland, Norway, Liechtenstein) agreed on a reduction of 21% of CO_2 emissions until 2020 compared to 2005. The system covers over 11,000 installations in the energy sector and electricity intense industries, such as steel, paper, cement industries etc. In total, about 45% of all EU emissions are limited by the EU ETS (EU Commission (January 2013)).

The EU ETS is based on the so-called *cap and trade* principle. The cap determines the total amount of greenhouse gas that can be emitted by all installations. After each year a company has to surrender enough *European Union Emission Allowances* (EUA) to cover their emissions. If more allowances are needed or if some remain unused, they can be freely traded among market participants. Hence, the emission reduction is performed where it is economically most senseful at lowest possible costs. If a company does not have enough EUAs to offset its pollution, a penalty of 100 € is charged. In addition, the allowance has to be handed in later, e.g. by reducing emissions in the next year or by buying it.

Due to the rapidly evolving emission markets, the amount of modelling approaches is steadily growing. Benz and Trück (2009) and Daskalakis et al. (2009) discuss a wide class of reduced form models, such as regime switching and models including jumps, which are common in computational finance, to approximate the CO_2 price dynamics of the EU ETS. As we want to link fundamental factors, such as fuel prices, to the price of carbon, we introduce a structural approach. It is closely connected to the one by Carmona et al. (2012), but we will deviate from their approach by modelling the CO_2 emission rate of the German market with the help of the framework of the previous chapters.

4.1 The CO_2 Emission Rate

The market emission rate μ_e is a positive and bounded function, which shall be influenced by the actual demand for energy, the available capacity and coal and gas prices. Furthermore, the emission rate shall react on changes in CO_2 allowance prices, which is basically the aim of the EU ETS. If carbon prices fluctuate, we expect a change in the merit order and hence a varying emission of greenhouse gas. To receive a feedback of EUA prices, we assume the electricity spot price to react towards changing prices. Due to the fact that generators have to buy certificates to offset their pollution and that they at least proceed any changes in production costs partially to the market, this assumption seems to be rather relevant. Nevertheless we could not find any empirical evidence for a linear relationship of allowance prices towards the density parameters within our data set. This may be explained by the low prices of CO_2 allowances during the years 2011 and 2012. In the sequel we assume a linear dependency of the form below to exist for the German market with the fuels coal and gas:

$$\mu_1 = \alpha_0 + \alpha_1 K + \alpha_2 G + \alpha_3 A, \qquad \sigma_1 = \beta_0 + \beta_1 K + \beta_2 G + \beta_3 A,$$
$$\mu_2 = \gamma_0 + \gamma_1 K + \gamma_2 G + \gamma_3 A, \qquad \sigma_2 = \delta_0 + \delta_1 K + \delta_2 G + \delta_3 A.$$

Furthermore, we assume that the emission costs are completely passed to the market. We therefore choose the sensitivities corresponding to Abadie and Chamorro (2008), IPCC (2006), VDI (2007):

$$\alpha_3 = \frac{e_1}{e_{ff_1}} = \frac{0.34056}{0.41425}\frac{tCO_2}{MWh}, \qquad \gamma_3 = \frac{e_2}{e_{ff_2}} = \frac{0.20196}{0.50625}\frac{tCO_2}{MWh}.$$

The parameter choice for $\beta_3 = \frac{\alpha_3}{10}$ and $\delta_3 = \frac{\delta_3}{10}$ is arbitrary. Since the intercept has been calibrated without any influence of carbon, we reduce it by the allowance sensitivity multiplied with the observed mean of EUAs of 10.3268 € / tCO_2. To be able to receive the current emission rate for the German market, we have to calculate how much energy is supplied by dirty generators. The percentage of clean energy is given by b_L. After these bids have been removed from the data set, $\hat{D}_t$ is the remaining demand which has to be fulfilled by conventional generators. With the help of model (3.1) and (3.2) respectively, we can calculate the percentage of the remaining demand, which is satisfied by generators of fuel $i = 1, 2$ via $w_i F_i(S_t)$ with $S_t = B(\frac{\hat{D}_t}{\hat{C}_t})$. Their contribution towards demand $\hat{D}_t$ is then given by $w_i F_i(S_t)\hat{C}_t$ for $i = 1, 2$. If we assume that each type of

generator has its specific emission rate $\hat{e}_i$ (tCO_2 / MWh), the overall emission rate is then

$$\mu_e(\hat{D}_t, A_t, M_t, K_t, G_t) = \hat{e}_1 w_1 F_1(S_t) \underbrace{(\hat{D}_t + M_t)}_{\hat{C}_t} + \hat{e}_2 w_2 F_2(S_t) \underbrace{(\hat{D}_t + M_t)}_{\hat{C}_t}.$$

In the sequel we will set $\hat{e}_1 = \frac{0.34056}{0.41425} \frac{tCO_2}{MWh}$, $\hat{e}_2 = \frac{0.20196}{0.50625} \frac{tCO_2}{MWh}$. The complexity of our emission rate can be reduced, if the margin process M_t is chosen to be deterministic. Thus we replace it by its seasonal, deterministic component $e^{s(t)}$ and write $\mu_e(\hat{D}_t, A_t, K_t, G_t) := \mu_e(\hat{D}_t, A_t, e^{s(t)}, K_t, G_t)$.

4.2 Emission Allowances

In this Section we want to price emission allowances as a derivative on the comulative emission. The cumulative emission can be gained by integrating the emission rate over time

$$E_t = \int_0^t \mu_e(\hat{D}_s, A_s, K_s, G_s) ds.$$

Thus we have

$$dE_t = \mu_e(\hat{D}_t, A_t, K_t, G_t) dt.$$

In combination with the underlying stochastic processes, we receive a four dimensional system of *stochastic differential equations* (SDE):

$$\begin{cases} d\hat{D}_t = \mu_{\hat{D}}(\hat{D}_t)dt + \sigma_{\hat{D}}(\hat{D}_t)dW_t, & \hat{D}_0 = \hat{d}_0 \in \mathbb{R}_+, \\ dK_t = \mu_K(K_t)dt + \sigma_K(K_t)d\hat{W}_{1,t}, & K_0 = k_0 \in \mathbb{R}_+, \\ dG_t = \mu_G(G_t)dt + \sigma_G(G_t)d\hat{W}_{2,t}, & G_0 = g_0 \in \mathbb{R}_+, \\ dE_t = \mu_e(\hat{D}_t, A_t, K_t, G_t)dt, & E_0 = 0. \end{cases}$$

Regarding the value of an EUA as a function of $A(t, \hat{D}_t, E_t, K_t, G_t)$, we can apply forward/backward SDE (FBSDE) theory to derive the following *partial differential equation* (PDE)

$$\begin{aligned} \frac{\partial A}{\partial t} + \mu_{\hat{D}}(\hat{D}) \frac{\partial A}{\partial \hat{D}} + \mu_e(\hat{D}, A, K, G) \frac{\partial A}{\partial E} + \mu_K(K) \frac{\partial A}{\partial K} + \mu_G(G) \frac{\partial A}{\partial G} \\ + \frac{1}{2}\sigma_{\hat{D}}(\hat{D})^2 \frac{\partial^2 A}{\partial \hat{D}^2} + \frac{1}{2}\sigma_K(K)^2 \frac{\partial^2 A}{\partial K^2} + \frac{1}{2}\sigma_G(G)^2 \frac{\partial^2 A}{\partial G^2} \\ + \rho \sigma_K(K)\sigma_G(G) \frac{\partial^2 A}{\partial K \partial G} - rA = 0, \end{aligned} \tag{4.1}$$

where r is the risk free interest rate. For more information on FBSDE and the derivation of the PDE we refer to Schwarz (2012) and Carmona et al. (2012). At maturity T one either has to pay the penalty π if cumulative emissions E exceed the emission cap E_{cap} or nothing if emissions have not reached the cap. So the allowance's payoff is given by

$$A(T, D, E, K, G) = \pi \mathbb{1}_{[E_{cap}, \infty)}(E). \tag{4.2}$$

A discussion of boundary conditions, needed to specify the solution, has been moved to Section 6. Please note that we price the emission permits under the historical measure $\mathbb{P}$ and neglect any influence of the market price of risk.

5 Case Studies

In this section we use our model to simulate several scenarios to analyse the effects of changes in the market environment. To be precise, we want to investigate how changes in exogenous factors, such as the emission cap, demand, capacity and fuel prices influence the electricity market, emission allowances and the value of conventional power plants. The scenarios will be compared to a base scenario, which can be considered as the business as usual market. In this scenario an emission cap of 20 million t/CO_2 is assumed. If the cap is exceeded during the trading period a penalty of 100€ is due. The starting prices of coal and gas are given by 100 USD/t (coal) and 25 €/MWh (gas), respectively. For the sake of simplicity we assume a fixed exchange rate of 1.30 USD = 1€ to convert the coal price to euro. The residual demand process starts at 2300 MWh. Tables 5.1, 5.2 summarize the used parameters and initial values. The spread options are computed for maturities $t = 1, ..., 8760$. To visualise our results and gain insights into the intra-day profitability of a power plant, we average option prices for all 24 trading hours of a day. Since there is no strong annual pattern in the German electricity market, we omit it in our analysis.

$\hat{D}_0$	K_0	G_0
2300	100	25

Table 5.1: Parameters base scenario

T	π	E_{cap}	r
8760	100	$20 * 10^6$	0.02

Table 5.2: Parameters EU ETS

5.1 Influence of the Emission Cap

In the year 2005 the EU started the EU ETS to fight the effects of the global climate change. Since then the price of EUAs has steadily declined. Critics argue that the number of emission permits has to be decreased to rekindle the carbon trading system. Within this scenario we want to analyse the impact of the emission cap on EUAs and in turn their influence on spread options for coal and gas fired power plants.

In Figure 5.1 (A) the price of EUAs is plotted for different emission caps and fixed fuel prices (100 USD/t and 25 €/MWh). The value at $x = 0$ represents the base scenario. Values at its right hand side stand for a generous emission cap and the values at the left hand side for a reduction of permits. If the cap is low and hence likely to be reached, the right to emit greenhouse gas is expensive. Vice versa, it is cheap if the cap is high. Figure (B) shows the emission reduction due to increasing EUA prices at different levels of capacity utilisation. If the capacity utilisation is low, gas plants can provide enough electricity to fulfill the complete demand and we see a reduction of 4.92% in emission. In the case of a high capacity utilisation dirty coal power plants are needed to fulfill demand, since there is not enough capacity from clean gas plants. Here the decrease in emitted CO_2 is only 2.57%. This emission reduction seems quite low, since it does not incorporate any changes in the total capacities of coal and gas generators. It can be interpreted as the short term effect of the emission trading system. In the long run we expect energy companies to change their power plant portfolio in favour of cleaner plants, if allowances remain at a high level. This results in a higher reduction of greenhouse gas emissions. Therefore, the model parameters have to be recalibrated if the market environment alters.

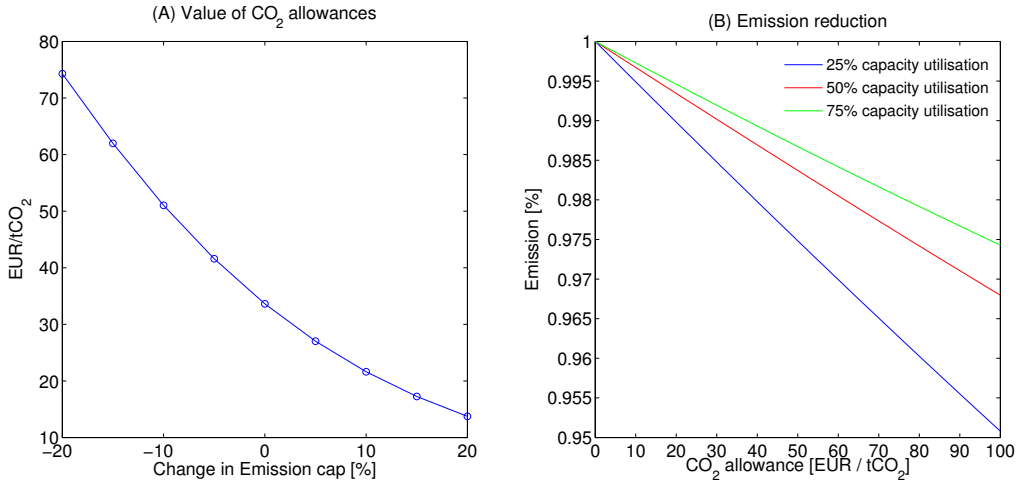

Figure 5.1: (A): Allowance value as a funtion of the emission cap
(B): Influence of allowances on the emission rate, $K = 100$, $G = 25$

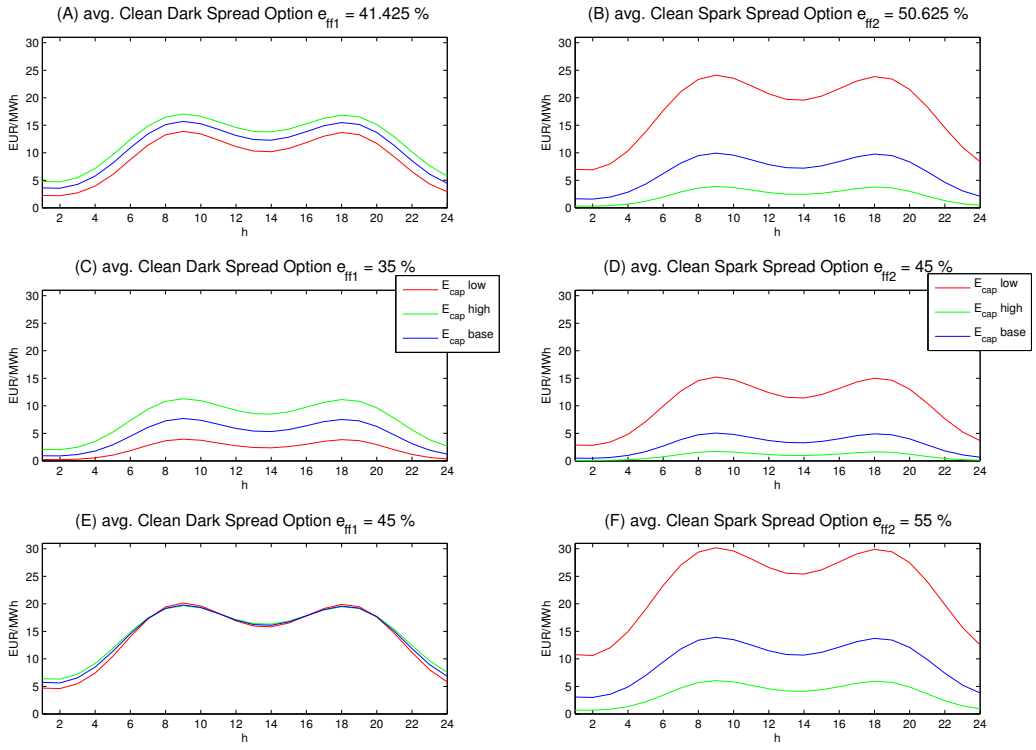

Figure 5.2: Influence of the emission cap

In Figure 5.2 we analyse the influence of the emission cap on coal and gas fired power plants. The spread options are computed for lowly, normally and highly efficient plants. The intra-day pattern with a top in the morning and another one in the evening corresponds to the demand cycle $\hat{D}$. The increase in demand leads to a higher price for electricity and thus to higher spreads. The value of a coal power plant shows adverse effects towards high allowance prices. Especially lowly efficient plants suffer from high prices, while highly efficient plants do not seem to be influenced. During periods of high demand, when the price for electricity is near the top of the stack, these cleaner power plants gain an extra profit by a price, which was set by less efficient coal plants. Hence, the negative effect of high carbon prices is compensated by an extra profit. Gas fired power plants are strongly influenced by the prices of emission allowances. If the cap is restrictive and hence the right to emit greenhouse gas is expensive, gas power plants are pushed in front of coal generators in the merit order. On the contrary they are behind coal generators in the merit order if allowances are cheap.

5.2 Influence of the Demand Process

In the second trading phase of the EU ETS, the European Union struggled into an economic recession. The lowered need for electricity led to a steady decline of emission certificates. In this case study, we want to simulate the effects of an economic boom and a recession. The boom will be modelled by a demand process, which is increased by 5% to simulate industrial prosperity and a strong need for energy. Vice versa, the depression is modelled by a drop in demand of 5%.

In Figure 5.3 we compare averaged clean spread options in the recession and boom scenarios. The higher need for energy in the boom scenario leads to a higher overall emission of greenhouse gas, hence, the allowances are more expensive. The starting values for EUAs are $A_0^{base} = 33.62$, $A_0^{+5\%} = 43.48$ and $A_0^{-5\%} = 24.86$. The boom scenario favours gas fired power plants in two points: the higher demand for energy pushes the price for electricity upwards and additionally carbon prices rise. Hence, we can see a strong impact of demand shifts on gas plants. In the case of coal plants rising EUAs have a negative effect. The plots reveal that the positive effects of increasing electricity prices on the one hand and adverse effects of rising EUAs on the other hand almost completely equate each other. In the case of lowly efficient coal plants, there is hardly any change in the spread options. The higher (lower) electricity price is almost completely compensated by higher (lower) carbon dioxide allowances.

5.3 Additional capacities by wind and solar power

In the lastest years the German federal government has encouraged the installation of renewables by subsidies in form of fixed prices and a guaranteed feed-in. In this case study we simulate the effects of additionally installed capacities by either solar or wind power. Since the EEG guarantees a feed-in, the demand that has to be fulfilled by conventional generators is lowered by the additionally provided capacity. Thus we expect a direct impact on the electricity spot price. Furthermore we expect to see a reduction of greenhouse gas emissions due to a greater share of renewables in the energy mix. In the following we perform a Monte Carlo simulation to compute the difference between the electricity spot price with and without additional feed-in. The additional capacities are simulated with the help of the processes defined in (3.6), (3.8). A lowered demand process is derived by subtracting the newly available capacities from the demand process $\hat{D}_t$. In order to incorporate the reduction of greenhouse gases, we solve the CO_2 allowance pricing PDE with respect to this new demand process. The randomness in the evolution of solar/wind capacities in (3.6), (3.8) is modelled via a stochastic driver. Doing so, one more dimension would be introduced into our allowance model -increasing the number of spatial dimensions from four to five. Since the curse of dimensionality shows its effect quickly for

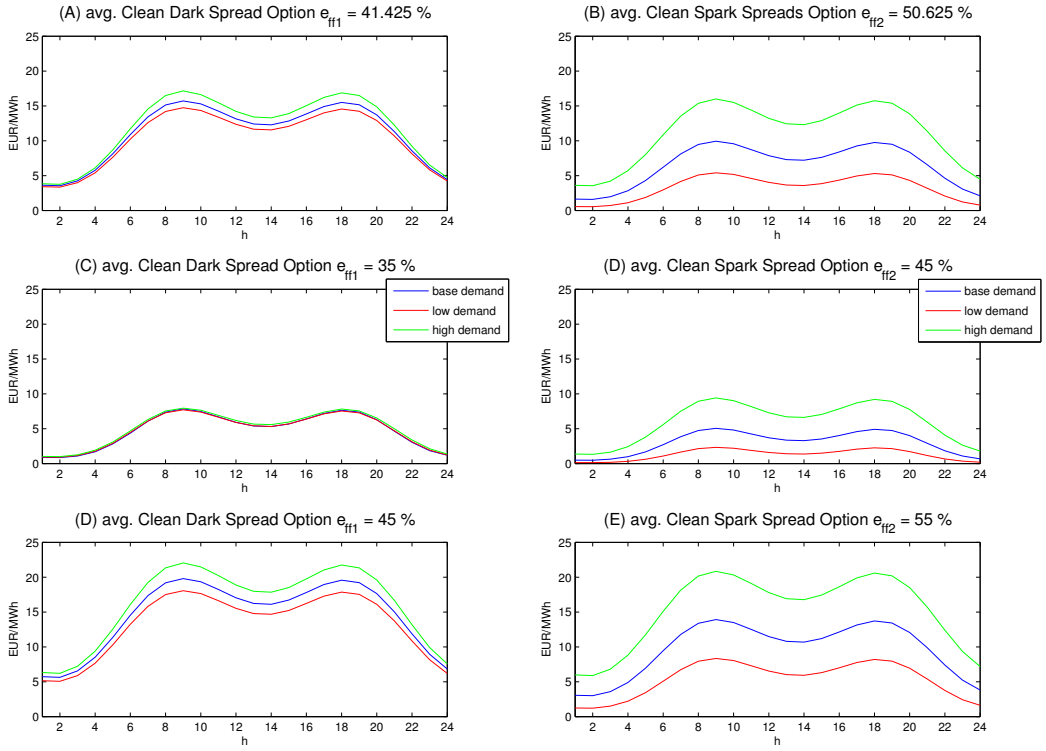

Figure 5.3: Influence of the demand

such high dimensional problems, we drop the stochastic component here and describe the feed-in by renewables with their deterministic component.

In Figure 5.4 the price drop of the electricity spot price due to additional feed-in by solar modules and wind power plants can be seen. The cleaner energy mix leads to a declining value of CO_2 allowances. If the feed-in is increased by one percent, the starting price of CO_2 allowances decreases from A_0=33.62 to $A_0 = 33.12$ (solar), $A_0 = 32.67$ (wind), respectively. The pattern follows the observed cycle in Section 3.5: In the case of solar power the price reduction is highest during midday when the sun is most powerful. During the night hours, the price reduction reflects the decrease in CO_2 allowance values. The additional wind feed-in leads to a peak in price reduction in the afternoon, which is in accordance to the intra-day feed-in pattern. Beside this we also find a reduction in the night hours. During these times the demand and capacity are very low. In this limited market environment any additional available capacity has a greater impact on the spot price for electricity than during high demand/capacity times.

We see that opposed to retail prices, which increase due to taxes to finance the German energy transition, the wholesale prices at the EPEX Spot market decline.

In the recent years an increase of the spot price volatility could be observed in the German energy market. Ketterer (2012) addresses this to the volatile nature of wind feed-in in combination with its direct influence on the electricity price. Our simulation results in Figure 5.5 confirm this behaviour. The volatility of baseload prices increases for a larger feed-in by wind. But this does not hold for more solar feed-in. Here the feed-in is not that volatile and we do not see a significant increase of the standard deviation of spot prices.

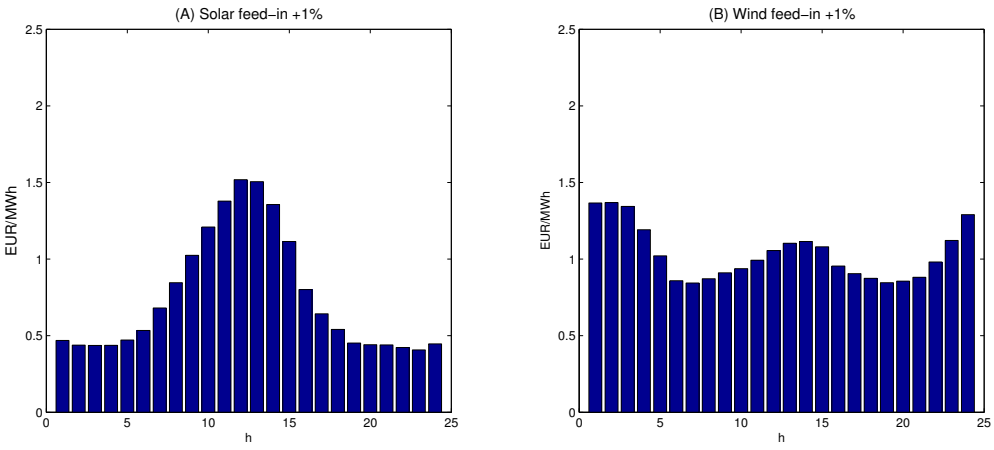

Figure 5.4: Electricity Spot Price Reduction due to additional feed-in by renewables

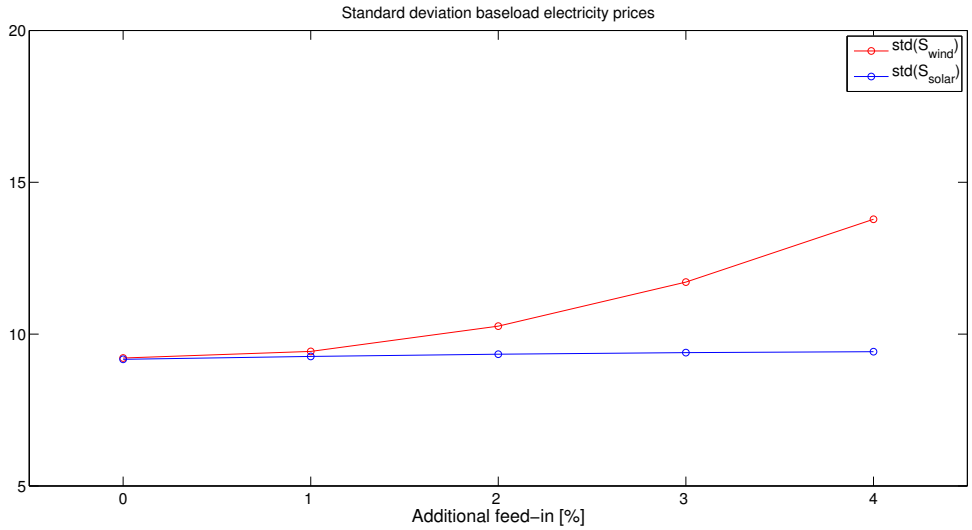

Figure 5.5: Standard deviation of baseload prices with additional feed-in from renewables

5.4 Influence of Changes in initial Fuel Prices

In the last years a drop in coal prices could be observed - favouring coal power plants and leading to more air pollution. In Figure 5.6 we see the emission rate and the allowance value in direction of both fuel processes for fixed values in demand and emission. High coal prices lead to an increased usage of gas fired power plants and thus to less pollution. Contrarily if gas is expensive, more coal power plants will be used and hence there is a higher emission of greenhouse gas. The allowance value exhibits the same form as the emission rate. If emission is high, there is a higher chance that the emission cap is reached and hence the certificate's value rises. In the

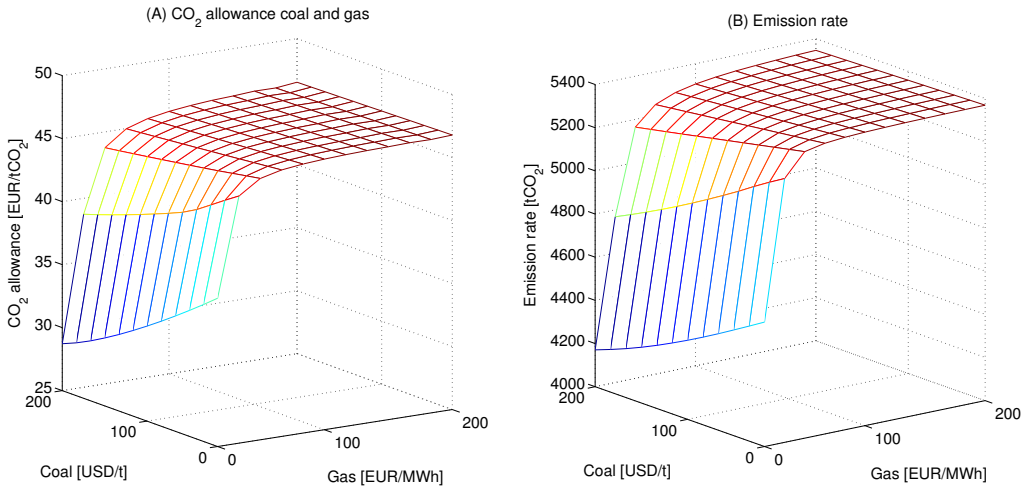

Figure 5.6: CO_2 allowance and emission in direction of coal and gas

following we want to simulate the influence of coal and gas prices on spread options. Since the fuel processes are mean reverting, this corresponds to a temporary shift in fuel prices. In the case of gas, we consider starting values of $G_0 = 15$ € / MWh and $G_0 = 35$ € / MWh. The mean reversion rate of $\theta_2 = 0.0026$ pushes the price back to its mean within approximately four months. In Figure 5.7 we see the spreads of normally, lowly and highly efficient plants with different gas starting values. In the case of a higher gas price the merit order effect favours coal fired power plants. As they are more likely to be online and produce electricity, they gain a higher profit. Vice versa coal power plants produce less energy if gas is cheap and the spread option value is lower. Gas fired power plants only show a slight influence on a change in initial gas prices. If gas prices are low, normally and highly efficient gas power plants can benefit from a shift in the merit order. During peak times, when gas power plants are the price setting technology, they can gain an extra profit if gas is expensive, as they move their bid level overproportional to changes in their production costs (cf. 3.2). Here, compared to the low gas prices case, the spread option value is higher.

In Figure 5.8 we compute the spreads with coal starting values $K_0 = 80$ USD / t and $K_0 = 120$ USD / t. Coal plant operators move their bid levels with a slope of 0.359,[2] while the production costs of an average plant move by 0.3448,[3] if the price of coal changes by one USD. Hence their margin remains rather stable if the coal price fluctuates. Although gas plants are behind coal plants at our simulated price levels in the bid stack, they gain an extra profit during peak times in demand, if coal and thus the price for electricity is high. Please note, that compared to Figure 5.7, the effects of changes in the initial coal price are stronger than for the gas price, since the coal process is less mean reverting.

[2] Please compare to Table 3.1.

[3] Assuming that coal burns at a rate of $7.00126 \frac{MWh}{t}$ and $e_{ff_1} = 41.425\%$: $\frac{1}{7.00126} \frac{1}{0.41425} = 0.3448$.

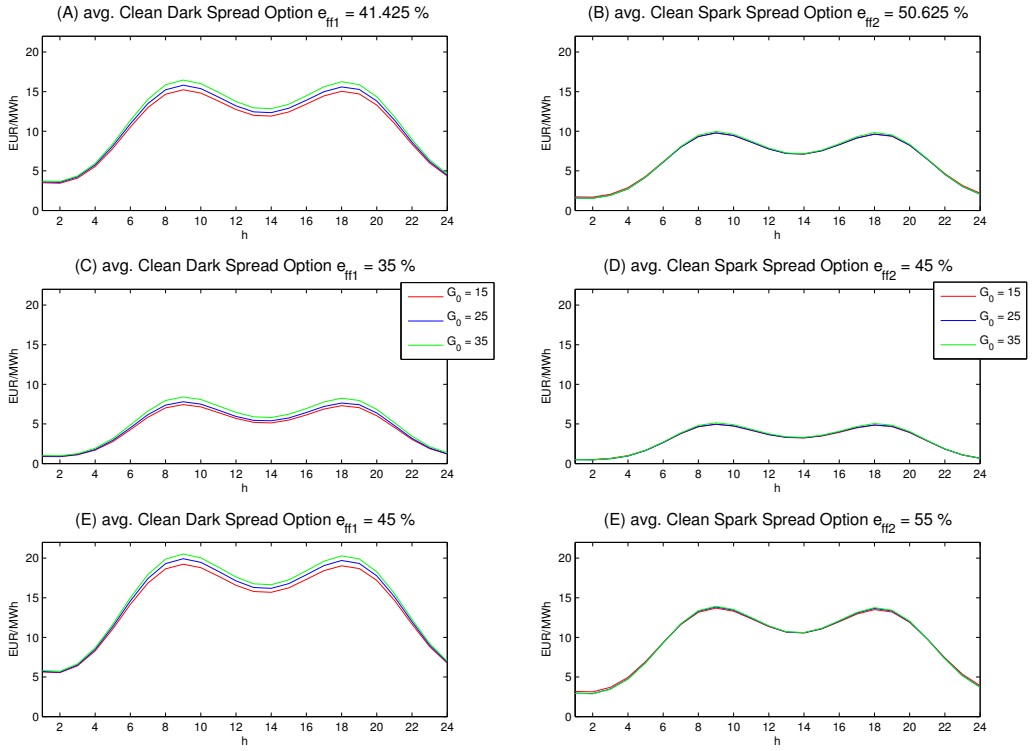

Figure 5.7: Influence of gas prices (base scenario)

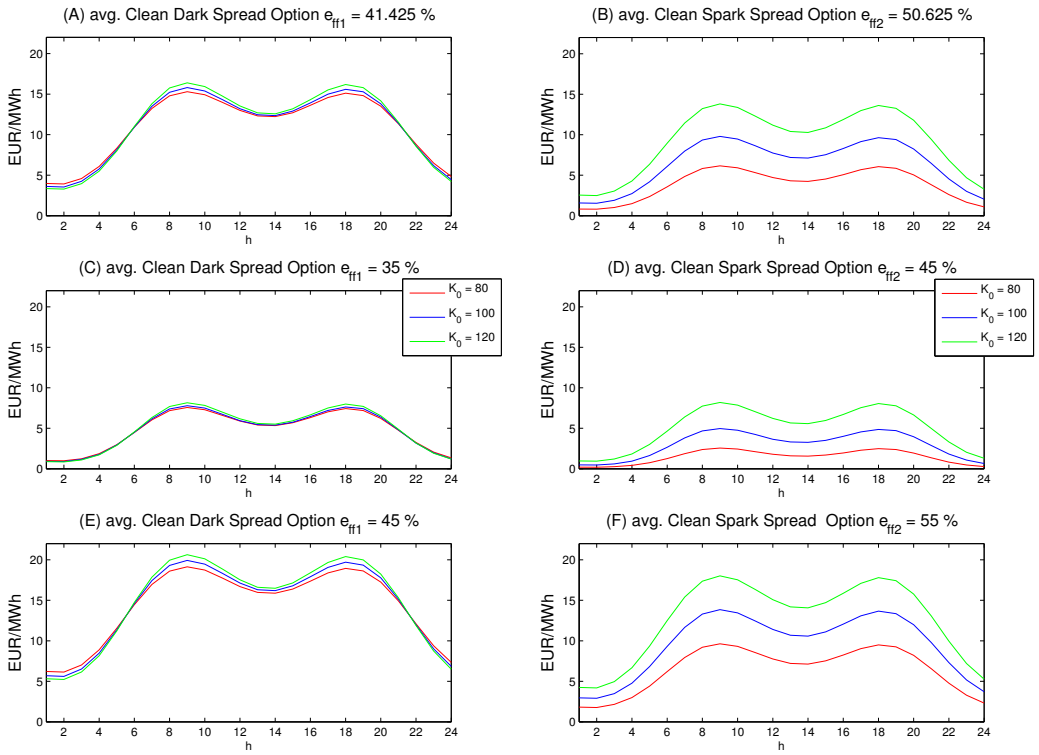

Figure 5.8: Influence of coal prices (base scenario)

6 Numerical Simulation

In this section we want to present numerical methods to solve the PDE (4.1) and to compute clean spread options.

6.1 Numerical Solution of EUAs

The PDE we want to solve numerically is given by (4.1)

$$\begin{aligned}\frac{\partial A}{\partial t}+\mu_d(t,D)\frac{\partial A}{\partial D}+\frac{1}{2}\sigma_d(D)^2\frac{\partial^2 A}{\partial D^2}+\mu_k(K)\frac{\partial A}{\partial K}+\frac{1}{2}\sigma_k(K)^2\frac{\partial^2}{\partial K^2}+\mu_g(G)\frac{\partial A}{\partial G}\\ +\frac{1}{2}\sigma_g(G)^2\frac{\partial^2 A}{\partial G^2}+\rho\sigma_k(K)\sigma_g(G)\frac{\partial^2 A}{\partial K\partial G}+\mu_e(D,A,K,G)\frac{\partial A}{\partial E}-rA=0\end{aligned}$$

with terminal condition at maturity $t=T$

$$A(T,D,E,K,G)=\pi\mathbb{1}_{[E_{cap},\infty)}(E).$$

The PDE shall be solved on the set $\Omega=(0,D_{max}]\times(0,E_{cap}]\times(0,K_{max}]\times(0,G_{max}]$ for all $t\in[0,T]$. We use the *Fichera function* to investigate if boundary conditions are necessary. A detailed introduction into *Fichera theory* can be found in Duffy and Kienitz (2009), Kichenassamy (2007). Let $\nu=(\nu_D,\nu_E,\nu_K,\nu_G)$ be the inward normal vector to the boundary $\partial\Omega$, then the *Fichera function* is defined on the part of the boundary, where the characteristic form is zero. The function is given by

$$\begin{aligned}b=&\left(\mu_d(D)-\frac{1}{2}\frac{\partial\sigma_d(D)^2}{\partial D}\right)\nu_D+\left(\mu_k(K)-\frac{1}{2}\frac{\partial\sigma_k(K)^2}{\partial K}-\frac{1}{2}\rho\sigma_g(G)\frac{\partial\sigma_k(K)}{\partial K}\right)\nu_K\\&+\left(\mu_g(G)-\frac{1}{2}\frac{\partial\sigma_g(G)^2}{\partial G}-\frac{1}{2}\rho\sigma_k(K)\frac{\partial\sigma_g(G)}{\partial G}\right)\nu_G+\mu_e(D,A,K,G)\nu_E.\end{aligned}$$

If $b<0$, the flow of information is inward and boundary conditions need to be specified. Contrarily if $b\geq 0$, the flow is outward and no boundary conditions are allowed. At the boundary $\partial\Omega$, which corresponds to $D=0$, $b\geq 0$ is fulfilled. At the lower boundary of both fuel processes $(K=0,G=0)$ the *Fichera function* is also positive. Since the emission rate μ_e is always positive and $\nu_E=-1$ at the boundary $E=E_{cap}$ the function is negative. Hence a boundary condition has to be specified. If the emission cap has already been reached, the penalty π surely has to be paid and the allowance value A is given by

$$A(t,D,E,K,G)=\pi e^{-r(T-t)}\text{ if }E\geq E_{cap}.$$

We discretise our five dimensional grid by

$$\begin{aligned}0<D_0<D_1<\cdots<D_{N_D-2}<D_{N_D-1}&=D_{max},\\0<K_0<K_1<\cdots<K_{N_K-2}<K_{N_K-1}&=K_{max},\\0<G_0<G_1<\cdots<G_{N_G-2}<G_{N_G-1}&=G_{max},\\0=E_0<E_1<\cdots<E_{N_E-2}<E_{N_E-1}&=E_{cap}-\Delta E,\\0=t_0<t_1<\cdots<t_{N_T-1}<t_{N_T}&=T,\end{aligned}$$

where $\Delta D=D_{i+1}-D_i$, $\Delta E=E_{j+1}-E_j$, $\Delta K=K_{k+1}-K_k$, $\Delta G=G_{g+1}-G_g$, $\Delta t=t_{n+1}-t_n$ for all i,j,k,g,n. In the following we want to simplify our notation and write

$$\begin{aligned}A^n_{i,j,k,g}&=A(t_n,D_i,E_j,K_k,G_g),\\\mu_{d;n,i}&=\mu_d(t_n,D_i),\\\sigma_{d;i}&=\sigma_d(D_i),\\\mu_{k;k}&=\mu_k(K_k),\\\sigma_{k;k}&=\sigma_k(K_k),\\\mu_{g;g}&=\mu_g(G_g),\\\sigma_{g;g}&=\sigma_g(G_g),\\\mu_{e;n,i,j,k,g}&=\mu_e(D_i,A^n_{i,j,k,g},K_k,G_g).\end{aligned}$$

The PDE will be solved numerically with the help of *Finite Difference Methods* (FDM). As the "curse of dimensionality" shows its effects very quickly in high dimensional problems, we try to lower the computational effort compared to standard FDM schemes. Standard schemes use broadly banded matrix equations, which are very expensive to solve. Alternating Direction Implicit (ADI) schemes avoid broad banded systems by decomposing them into simpler tridiagonal matrices. These can be solved efficiently by LU-decomposition. More information can be found in Duffy (2006), Haentjens and Hout (2012). In order to simplify our notation, we will use an operator notation in our scheme:

$$\begin{aligned}
\delta_x^+ u(x) &= u(x+\Delta x) - u(x) \\
\delta_x^- u(x) &= u(x) - u(x-\Delta x) \\
\delta_x^0 u(x) &= u(x+\Delta x) - u(x-\Delta x) \\
\delta_x^2 u(x) &= u(x+\Delta x) - 2u(x) + u(x-\Delta x) \\
\delta_x^0 \delta_y^0 u(x,y) &= u(x+\Delta x, y+\Delta y) - u(x-\Delta x, y+\Delta y) \\
&\quad - u(x+\Delta x, y-\Delta y) + u(x-\Delta x, y-\Delta y)
\end{aligned}$$

The scheme we use is given by

$$\begin{aligned}
&\left(1 + \frac{1}{2}r\Delta t - \frac{1}{2}\mu_{d;n+\frac{1}{2},i}\frac{\Delta t}{\Delta D}\delta_D^{+/-} - \frac{1}{4}\sigma_{d,i}^2\frac{\Delta t}{\Delta D^2}\delta_D^2\right)\Delta A^* = \Bigg(- r\Delta t + \mu_{d;n+\frac{1}{2},i}\frac{\Delta t}{\Delta D}\delta_D^{+/-} + \frac{1}{2}\sigma_{d;i}^2\frac{\Delta t}{\Delta D^2}\delta_D^2 \\
&\qquad + \mu_{k;k}\frac{\Delta t}{2\Delta K}\delta_K^0 + \frac{1}{2}\sigma_{k;k}^2\frac{\Delta t}{\Delta K^2}\delta_K^2 + \mu_{g;g}\frac{\Delta t}{2\Delta G}\delta_G^0 + \frac{1}{2}\sigma_{g,g}^2\frac{\Delta t}{\Delta G^2}\delta_G^2 \\
&\qquad + \mu_{e;n+1,i,j,k,g}\frac{\Delta t}{\Delta E}\delta_E^+ + \rho\sigma_{k;k}\sigma_{g;g}\frac{\Delta t}{4\Delta K\Delta G}\delta_K^0\delta_G^0\Bigg)A^{n+1} \\
&\left(1 - \frac{1}{2}\mu_{k;k}\frac{\Delta t}{2\Delta K}\delta_K^0 - \frac{1}{4}\sigma_{k;k}^2\frac{\Delta t}{\Delta K^2}\delta_K^2\right)\Delta A^{**} = \Delta A^* \\
&\left(1 - \frac{1}{2}\mu_{g;g}\frac{\Delta t}{2\Delta G}\delta_G^0 - \frac{1}{4}\sigma_{g;g}^2\frac{\Delta t}{\Delta G^2}\delta_G^2\right)\Delta A^{***} = \Delta A^{**} \\
&\left(1 - \frac{1}{2}\mu_{e;n+1,i,j,k,g}\frac{\Delta t}{\Delta E}\delta_E^+\right)\Delta A = \Delta A^{***}
\end{aligned} \tag{6.1}$$

with $\Delta A = A^n - A^{n+1}$. This scheme can be derived by factorizing a Crank-Nicolson scheme and rewriting the system in the so-called **delta formulation** (Thomas (1998)). According to Craig and Sneyd (1988), Haentjens and Hout (2012) the mixed derivative is treated explicitly. Please note that $n+1$ designates the explicit part, since we are stepping backwards in time. In direction of demand we use an upwind scheme in the convective part to account for a high **Péclet number**. In direction of both fuel processes no convection dominance can be found and hence central differences are deployed to approximate the first derivative. In order to handle the non-linearity in the emission drift function, the allowance value of the previous step is used. Since the feedback of its price on the emission rate is rather moderate (cf. Section 5.1), we do not expect to introduce a large error. In the last leg we have to determine the boundary condition in the artificial variable ΔA. Since ΔA is the difference in an allowance value of two consecutive time steps, we choose the boundary condition as

$$\Delta A = \pi\left(e^{-r(T-t_n)} - e^{-r(T-t_{n+1})}\right) \text{ if } E_t \geq E_{cap}.$$

A detailed discussion of the stability, consistency and convergence properties can be found in Hendricks (2013).

6.2 Monte Carlo Simulation of Clean Spread Options

The clean spread options in Section 2 are computed via *Monte Carlo Simulations*. The underlying paths D, K and G are simulated with the analytic solution of an Ornstein-Uhlenbeck process,

while we use a *Euler scheme* to approximate the evolution of cumulative emission. The EUA value is received by interpolating the discrete solution from our FDM scheme. As a tradeoff between accuracy and speed, a linear interpolation routine is used.

The option value is estimated by simulating N payoffs and paths, respectively, with maturity T

$$\hat{V}_{CDS} = e^{-rT} \frac{1}{N} \sum_{i=1}^{N} \left(S_T^i - \tfrac{1}{e_{ff_1}} \left(K_T^i + e_1 \, A_T^i \right) \right)^+ ,$$

$$\hat{V}_{CSS} = e^{-rT} \frac{1}{N} \sum_{i=1}^{N} \left(S_T^i - \tfrac{1}{e_{ff_2}} \left(G_T^i + e_2 \, A_T^i \right) \right)^+ ,$$

where the index i denotes the i-th simulated path and S is derived by solving equation (3.2).

7 Conclusion

In this paper we have introduced a coupled model for electricity and EUA prices in the German electricity market. Based on a stochastic bid stack function, which connects demand and fuel with the electricity price, we have analysed EPEX Phelix bid data. The high supply from renewable energy and the regulations, concerning the forced usage of green energy, make the German energy market relatively unique in the world. The bid stack function could be extended to cope with the singularities of the German market. Furthermore, we have introduced the price of EUAs as an additional price driver. Building on the bid stack model, we implemented an emission rate, which connects fundamental factors and emission in a reasonable way.

The value of EUAs could be evaluated by solving a PDE with four spatial dimensions. It was solved numerically by an ADI scheme, based on a Crank-Nicolson approximation. With the help of our model it could be shown that the price reduction effect of renewables is two-fold. On the one hand due to a lowered residual demand and on the other hand due to a declining value of emission permits. Beside the price damping effect the installation of wind capacities also increased the spot market volatility, leading to more risk for market participants. The computation of clean spread options turned out that the spread significantly depends on the emission cap, the demand for electricity, the fuel prices and on the efficiency of a certain power plant. If the cap is determined carefully, thus leading to a working carbon market, clean plants are pushed forward in the merit order. The values of dirty and inefficient power plants drop to low levels and the incentive to invest in new technologies or switch to a cleaner fuel rises. In the high demand scenario, gas power plants could greatly benefit from higher electricity and EUA prices. In the last case study we have analysed the influence of changes in initial fuel prices. Although the fuel processes are mean reverting, we could see an influence on the value of power plants. Opposed to our intuitive expectation that gas power plants profit from declining gas prices, the simulations showed that this does not hold. Their value is much more influenced by the bids of their competitors (coal power plants).

Acknowledgement

We would like to thank the anonymous referee for his helpful comments and valuable suggestions.

References

L.M Abadie and J.M Chamorro. Carbon price risk and the clean dark spread. http://www.fae1-eao1.ehu.es/s0043-con/en/contenidos/informacion/00043_seminarios/es_00043_se/adjuntos/Chamorro_Spread.pdf, 2008.

BDEW. Erneuerbare Energien und das EEG: Zahlen, Fakten, Grafiken (in german), 2011.

E. Benz and S. Trück. Modeling the price dynamics of CO_2 emission allowances. *Energy Economics*, 31:4–15, 2009.

H. Bessembinder and M. L. Lemmon. Equilibrium pricing and optimal hedging in electricity forward markets. *Finance*, 27:1347–1382, 2002.

BMU. Erneuerbare Energien - Innovationen für die Zukunft. http://www.dlr.de/Portaldata/41/Resources/dokumente/institut/system/publications/broschuere_ee_innov_zukunft.pdf, 2004.

R. Carmona, M. Coulon, and D. Schwarz. The valuation of clean spread options: Linking electricity, emissions and fuels. *Quantitative Finance*, 12:1951–1965, 2012.

European Commission. *The EU Emission Trading System (EU ETS).* European Comission, January 2013.

I.J.D. Craig and A.D. Sneyd. An alternating-direction implicit scheme for parabolic equations with mixed derivatives. *Comput. Math. Appl.*, 16.4:341–350, 1988.

M. Culot, V. Goffin, S. Lawford, S. de Menten, and Y. Smeers. Practical stochastic modeling of electricity prices. *Energy Markets*, 6(1):3–31, 2013.

G. Daskalakis, D. Psychoyios, and R.N. Markellos. Modeling CO_2 emission allowance prices and derivates: Evidence from the European trading scheme. *Banking and Finance*, 33:1230–1241, 2009.

C. DeJong. The nature of power spikes: A regime-switch approach. *The Berkeley Electronic Press*, 10(3), 2006.

D.J. Duffy. *Finite Difference Methods in Financial Engineering: A Partial Differential Equation Approach.* Wiley Finance, 2006.

D.J. Duffy and J. Kienitz. *Monte Carlo Frameworks: Building Customisable High-performance C++ Applications.* Wiley Finance, 2009.

EPEXSpot. Description of indices derived from epex spot markets. http://static.epexspot.com/document/12852/EPEXSpot_Indices.pdf, 2012.

A. Eydeland and K. Wolyniec. *Energy and Power Risk Management: New Developments in Modeling, Pricing, and Hedging.* John Wiley & Sons, 2002.

T. Haentjens and K. J. In't Hout. Alternating direction implicit finite difference schemes for the heston–hull–white partial differential equation. *Comput. Finance*, 16:83–110, 2012.

Heizung-Direkt. Heat of combustion. http://www.heizung-direkt.de/UEBERSHO/brennwert.htm, 2013.

C. Hendricks. Modelling and numerical simulation of clean spark spread options in the German electricity market. Master's thesis, Bergische Univerität Wuppertal, 2013.

S. Howison and M. Coulon. Stochastic behaviour of the electricity bid stack: From fundamental drivers to power prices. *Energy Markets*, 2(1), 2009.

IPCC. Ipcc guidelines for national greenhouse gas inventories, 2006.

J.C. Ketterer. *The impact of Wind Power Generation on the Electricity Price in Germany. Ifo Working Paper*, 143, 2012.

S. Kichenassamy. *Fuchsian Reduction: Applications to Geometry, Cosmology and Mathematical Physics (Progress in Nonlinear Differential Equations and Their Applications)*. Birkhäuser, 2007.

W. Margrabe. The value of an option to exchange one asset for another. *Finance*, 1978.

D. Schwarz. Price modelling and asset valuation in carbon emission and electricity markets. *PhD. Thesis*, 2012.

L. Teng, C. van Emmerich, M. Ehrhardt, and M. Günther. A general approach for stochastic correlation using hyperbolic functions. *Preprint Wuppertal*, 2013.

J.W. Thomas. *Numerical Partial Differential Equations - Finite Difference Methods*. Springer, 1998.

VDI. CO_2-Emission der Stromerzeugung (in german). http://www.vdi.de/fileadmin/vdi_de/redakteur_dateien/geu_dateien/FB4-Internetseiten/CO2-Emissionen%20der%20Stromerzeugung_01.pdf, 2007.